Journal of Materials Chemistry A

RSC Publishing

PAPER

View Article Online
View Journal | View Issue

Nano-structured carbon-coated CuO hollow spheres as stable and high rate anodes for lithium-ion batteries

Cite this: *J. Mater. Chem. A*, 2013, **1**, 15486

Yunhua Xu,†[a] Guoqiang Jian,†[b] Michael R. Zachariah*[ab] and Chunsheng Wang*[a]

Received 15th September 2013
Accepted 25th October 2013

DOI: 10.1039/c3ta13698a

www.rsc.org/MaterialsA

Carbon-coated CuO hollow spheres with a thin layer of CuO nanoparticles anchored to the outer carbon layer were synthesized using a one-step, fast, scalable, and low-cost aerosol spray pyrolysis method. The hollow spherical particles provide a capacity of 670 mA g^{-1} at 1 C and maintain the capacity for 300 cycles and 400 mA h g^{-1} at 50 C. This is the best performance for CuO anodes reported to date. The exceptional electrochemical performance is attributed to the unique architecture of the carbon-coated hollow structure.

Introduction

Lithium-ion batteries have been considered as a promising power source for electric vehicles and grid energy storage. However, the current battery technology, which uses graphite anodes and shows a low theoretical capacity of 372 mA h g^{-1}, cannot meet the requirement of high power and high energy for the next generation rechargeable batteries.[1] New anode materials with high power, high capacity, good cycling stability, as well as low cost and non-toxic nature are desired. Transition metal oxides, such as Fe_2O_3, CuO, NiO, Co_3O_4 and MnO_2, have been demonstrated to have high capacity through conversion reaction with lithium ions.[2–5]

Among these metal oxides, CuO has attracted considerable attention as a promising anode material because of its high theoretical capacity (674 mA h g^{-1}), low cost and its nontoxic nature.[6–10] However, the realization of high capacity and high rate capability for CuO anodes has been impeded by the severe volume change during the conversion reaction with lithium ions, and its low conductivity. Recently, to circumvent these issues, nanostructures and incorporation of carbon materials have been developed and demonstrated with improved electrochemical performance.[11–17] Unfortunately, real success in long cycle life and high rate capability has not been achieved for CuO anode materials.

Although nanomaterials can alleviate mechanical strain and reduce the diffusion length of Li ions, the large surface area of nanoparticles (NPs) requires much more conductive additives to maintain the activity.[18] In addition, the large amount of accumulated solid electrolyte interface (SEI) films resulting from the decomposition of the electrolyte upon volume change during repeated cycles isolate the nanoparticles, thus losing their activity. Recently, Ko *et al.* reported CuO/MWCNT nanocomposites, in which the mesoporous CuO particles are threaded with CNTs in the long-axis direction.[9] Enhanced rate capability was observed as a result of the use of CuO nanostructures, CNT conductive networks, as well as the strong binding interaction between NPs and CNTs.

It is clear that the ideal structure of CuO should have (1) nano-size to mitigate volume change and decrease diffusion length of Li ions to improve cycling stability; (2) a conductive network (such as graphene, carbon nanotubes and amorphous carbon) to provide a continuous electron transportation pathway to enhance conductivity; (3) good contact between CuO NPs and the conductive network to maintain the electrochemical activity of CuO nanoparticles. However, uniform incorporation of carbon into CuO materials using conventional methods is a significant challenge due to the reduction property of carbon at high temperature.

In this paper, we successfully coated carbon onto CuO hollow spheres, in which the CuO nanowalls are formed by a layer of CuO NPs (~10 nm) and these CuO NPs are anchored to the outer layer of carbon (Fig. 1 and 2). Carbon coated CuO hollow nanospheres were prepared using a one-step, fast, scalable, and low-cost synthesis method, aerosol spray pyrolysis, which enables us to rapidly heat micron sized precursor droplets to high temperature followed by a fast cooling process.[19] Short residential time (a few seconds) allows quick formation of CuO NPs and fast carbonization to avoid the reduction of CuO. The carbon coated CuO hollow spheres demonstrated exceptional electrochemical performance, high capacity, excellent rate capability and long-term cycling stability.

[a]*Department of Chemical and Biomolecular Engineering, University of Maryland, College Park, MD 20742, USA. E-mail: cswang@umd.edu*

[b]*Department of Chemistry and Biochemistry, University of Maryland, College Park, MD 20742, USA. E-mail: mrz@umd.edu*

† These authors contributed equally to this work.

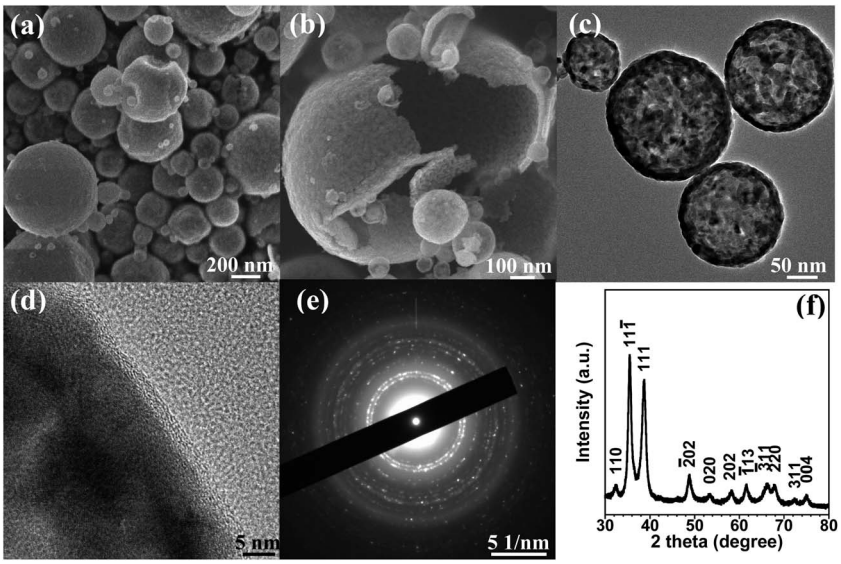

Fig. 1 (a and b) SEM, (c and d) TEM, (e) SAED images and (f) XRD spectrum of the nano-structured carbon-coated CuO hollow spherical particles.

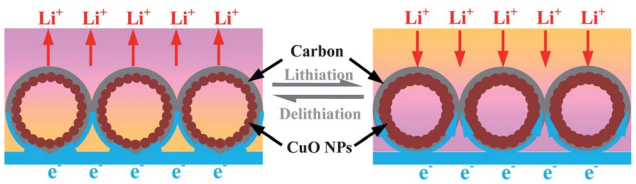

Fig. 2 Schematic illustration of structure change during the charge/discharge processes of the nano-structured carbon-coated CuO hollow spherical particles.

Experimental section

Synthesis of carbon-coated hollow CuO spheres

The synthesis of carbon-coated hollow CuO spheres is similar to the synthesis of hollow CuO spheres as described in our previous publication.[19] The difference is that the precursor solution with higher concentration of copper nitrate and sucrose was used to enable partial carbonization of sucrose and thus to form a carbon layer on CuO particles. In detail, 2.89 g of copper nitrate trihydrate ($Cu(NO_3)_2 \cdot 3H_2O$, Strem Chemical), 0.51 g of sucrose ($C_{12}H_{22}O_{11}$, Sigma-Aldrich) and 15 mL of hydrogen peroxide solution (30 wt%. H_2O_2, Sigma-Aldrich) were dissolved into 45 mL of distilled water. The prepared precursor solution was atomized with a homemade collision-type atomizer using compressed air at a pressure of 0.24 MPa. The atomized aerosol droplets were passed through a silica-gel diffusion dryer first to remove the most of the solvent and then a tube furnace set at 600 °C. The normal residence time was estimated to be around 1 s for a total gas flow rate of 3.5 L min^{-1}. The produced product was collected on a HTTP Millipore filter (pore size: 0.4 μm).

Material characterization

Scanning electron microscopy (SEM) and transmission electron microscopy (TEM) images were taken using a Hitachi SU-70 analytical ultra-high resolution SEM (Japan) and JEOL 2100F field emission TEM (Japan), respectively. The X-ray diffraction (XRD) pattern was recorded using a Bruker Smart1000 (Bruker AXS Inc., USA) using CuKα radiation.

Electrochemical measurements

The carbon-coated hollow CuO spheres were mixed with carbon black and sodium carboxymethyl cellulose (CMC) binder to form a slurry at a weight ratio of 70 : 15 : 15. The electrode was prepared by casting the slurry onto copper foil with an active material loading of 0.5–1 mg cm^{-2} using a doctor blade, and dried in a vacuum oven at 100 °C overnight. Coin cells were assembled with lithium foil as the counter electrode, 1 M $LiPF_6$ in a mixture of ethylene carbonate–diethyl carbonate (EC–DEC, 1 : 1 by volume) as the electrolyte, and Celgard®3501 (Celgard, LLC Corp., USA) as the separator. Electrochemical performance was tested using Arbin battery test station (BT2000, Arbin Instruments, USA). Rate capability was examined by charging–discharging at different rates (C rate = 670 mA g^{-1}). The cyclic voltammogram scanned at 0.1 mV s^{-1} between 0 and 3 V was recorded using a Solatron 1260/1287 Electrochemical Interface (Solartron Metrology, UK). For comparison, the commercial CuO nanoparticles with a particle size of 50 nm (Sigma-Aldrich) were examined under the same cell assembly and test conditions.

Results and discussion

In the aerosol spray pyrolysis process, the solution of copper nitrate was atomized to form small droplets and then thermally decomposed to form CuO NPs. Meanwhile, sucrose and hydrogen peroxide (H_2O_2) in the precursor solutions functioned as gas blowing agents to promote the formation of large hollow architectures. More importantly, by tuning the concentration of sucrose and H_2O_2 in the precursor aerosol droplets, partial

carbonization of sucrose can be achieved to form carbon coated CuO hollow particles. Totally different from the previous reports on C/CuO composites that were normally prepared at a low temperature to avoid reduction of CuO by carbon,[6,9,14] the aerosol spray pyrolysis process provides rapid heating of micron sized precursor droplets to a high temperature (600 °C or higher) in an oxidation environment (air and H_2O_2), allowing quick formation of CuO nano-grains, partial carbonization of carbon sources, and generation of gas to form a hollow structure. The short residence time at a high temperature and subsequent fast cooling in an oxidizing environment ensures a rapid precursor decomposition process, thus preventing the reduction reaction.

The morphology and architecture of the carbon-coated CuO hollow spheres were characterized using scanning electron microscopy (SEM) and transmission electron microscopy (TEM). As shown in the SEM image in Fig. 1a, the carbon-coated CuO hollow spheres preserved the spherical morphology of the atomized precursor droplets, while the image of the broken particles (Fig. 1b) revealed their hollow structure. It is also clear that the wall of the hollow particles consists of a thin layer of NPs with a diameter of ~10 nm. The hollow structure of CuO is further confirmed by the TEM image in Fig. 1c. The high-resolution TEM (HRTEM) image in Fig. 1d clearly shows that the hollow particles were coated with an ultra-thin layer of carbon (~3 nm). Thermogravimetric analysis (TGA) revealed that the carbon content is less than 3 wt%. The selected area electron diffraction (SAED) image in Fig. 1e presents well-defined diffraction rings, indicating that the CuO NPs have a crystalline structure. The crystalline nature of CuO is confirmed by the X-ray diffraction (XRD) spectrum shown in Fig. 1f, which can be indexed to the monoclinic CuO (JCPDS no. 48-1548).

The unique structure of the carbon-coated CuO hollow spherical particles has a number of advantages as an anode material for lithium-ion batteries. Firstly, the ultra-small NPs efficiently reduce not only the stress/strain caused by the volume change during the insertion/extraction processes but also the ion diffusion length within the active particles, facilitating the cycling stability and charge transfer reaction. Secondly, the void space in the hollow spheres can accommodate the large volume change induced by chelation reactions. Thirdly, the thin layer CuO nanoparticle structure that is sealed by a carbon layer blocks the penetration of the electrolyte into the centre hole reducing the irreversible capacity. Fourthly, the thin carbon coating layer provides a mechanical support to maintain the integrity of the CuO NPs upon repeated cycles. Finally, the thin layer of carbon also serves as an electron transportation pathway, enhancing the electrical conductivity of the electrode. The functions are illustrated schematically in Fig. 2. Therefore, long cycling stability and high rate capability are anticipated for nano-structured carbon-coated CuO hollow spheres.

Fig. 3a shows the cyclic voltammogram (CV) curves of the carbon-coated CuO hollow spheres in the initial 5 cycles between 0 and 3 V at a scan rate of 0.1 mV s^{-1}. In the first cathodic scan, three peaks were observed at 1.90, 1.12, and 0.88 V, corresponding to the formation of a solid solution of

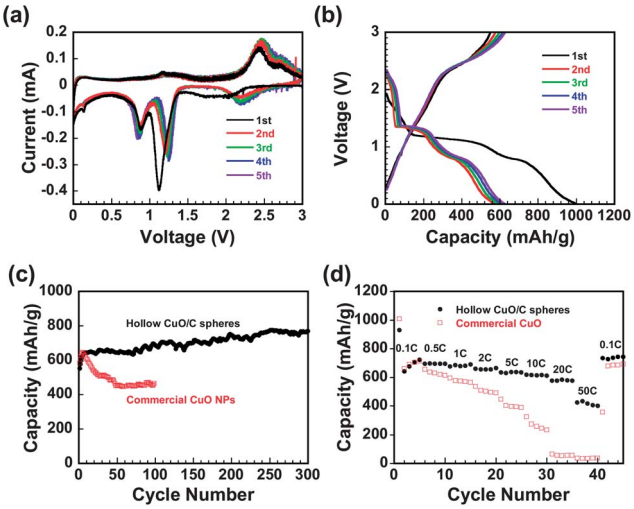

Fig. 3 Electrochemical performance of the nano-structured carbon-coated CuO hollow spherical particles and commercial CuO NPs. (a) CV curves, (b) charge/discharge profiles, (c) cycling stability, and (d) rate capability.

$Cu_{1-x}{}^{II}Cu_x{}^{I}O_{1-x/2}$, a phase transition into Cu_2O, and the formation of Cu nanograins dispersed into a lithia matrix (Li_2O), respectively.[20] In the following scans, the current peaks at 1.12 and 1.90 V shift to and maintained at higher potentials of 1.20 and 2.20 V, respectively. The potential shift to more positive potential in the second cycle is a common phenomenon for metal oxide anodes and was attributed to the structure changes during the lithium-ion insertion in the first lithiation.[21] The higher peak current in the first lithiation was partially attributed to the formation of solid electrolyte interface (SEI) films. There is no obvious difference in the anodic scans in the first five cycles. The almost identical lithiation/delithiation behaviour after the second cycle demonstrates good reversibility and stability of the carbon-coated CuO hollow spheres.

Fig. 3b shows the charge–discharge profiles of the carbon-coated CuO hollow spheres in the first 5 cycles. It provides a lithiation capacity of 1003 mA h g^{-1} and a reversible capacity of 551 mA h g^{-1}, corresponding to a coulombic efficiency of 55%, which is higher than a previous report on CuO/C composite anodes.[22] The irreversible capacity is mainly associated with the formation of SEI films. In the following cycles, the capacity slightly increases and the coulombic efficiency approaches 100%.

The cycling performance of the carbon-coated CuO hollow spheres was examined by charge–discharge cycles between 0 and 3.0 V at a 1 C rate (670 mA g^{-1}). For comparison, commercial CuO NPs with an average particle size of 50 nm were also examined under the same conditions. As shown in Fig. 3c, the charge capacity of carbon-coated CuO hollow spheres quickly increased from 550 mA h g^{-1} to ~640 mA h g^{-1} in the first five cycles, and then gradually increased to about 750 mA h g^{-1} in the 300th cycle. This is much better than those reports on CuO anodes in the literature. The capacity increase during charge–discharge cycles has also been reported on several metal and metal oxide anodes (Sn,[23] Fe_2O_3,[24] CoO,[25] and CuO,[20,26]). Some of them show higher capacity than their

theoretical values. The extra capacity is normally attributed to the reversible formation of gel-like polymeric species in the SEI films due to the catalytic activity of metals in the anodes.[20,23–26] In this case, the continuous increase in capacity over 300 cycles demonstrates that the volume change of the CuO anodes during the lithium-ion insertion/extraction may build more reversible polymeric species, and thus contributing more extra capacity. The commercial CuO NPs delivered a similar capacity to the carbon-coated CuO hollow spheres in the initial few cycles, but they suffered a rapid capacity decay to ~450 mA h g^{-1} after 50 cycles. These results clearly demonstrate the superior cycling performance of the nano-structured carbon-coated CuO hollow spheres over the commercial NPs.

The rate capability of the nano-structured carbon-coated CuO hollow spheres and the commercial NPs was investigated by charging (delithiation) at 0.1 C and discharging (lithiation) at different C rates (Fig. 3d). The nano-structured carbon-coated CuO hollow spheres also demonstrated excellent discharge rate capability. Even at a very high rate of 50 C (3.35 A g^{-1}), it still retained as high as 400 mA h g^{-1}, which means that the carbon-coated CuO hollow sphere anodes can be discharged in 1.2 minutes with higher capacity retention than graphite anodes. To date, this is the best rate performance for CuO anodes we are aware of. In contrast, the commercial CuO NPs failed to provide capacity at 20 C. It was noticed that when the current was changed back to 0.1 C, the commercial CuO NP anodes almost recovered their initial capacity. The reason is possibly that at low current, the commercial CuO NPs can be fully lithiated and delithiated, resulting in large volume change and severe structure deformation; while at high current density, the low conductivity of commercial CuO NPs induces a large overpotential, thus only partial CuO NPs are lithiated/delithiated, and small volume change and less structure deformation are induced. The less volume change of commercial CuO NPs at a high rate can extend the cycling stability. Therefore, the cycling stability of commercial CuO NPs at a high C rate should be better than that measured at a low C rate. This is the reason why the capacity retention of the commercial CuO NPs at 0.1 C after an aggressive rate test from 1 C to 50 C for 40 cycles (Fig. 3d) is higher than the capacity retention of commercial CuO NPs after 40 cycles at 1 C (Fig. 3c). The excellent discharge capability of the nano-structured carbon-coated CuO hollow spheres demonstrated a significant advance in Li-ion battery technologies because the discharge power density is critical for most practical applications. The exceptional electrochemical performance is attributed to the unique structure of the nano-structured carbon-coated hollow particles.

The morphology changes of the nano-structured carbon-coated CuO hollow particles after 70 charge–discharge cycles between 0 and 3.0 V at 1 C were investigated using SEM (Fig. 4). Most hollow CuO particles preserved the spherical morphology and the architecture of the as prepared samples (Fig. 1). Few collapsed particles may be attributed to the mixing/coating process. The integrity of the thin layer of CuO NPs was still maintained (Fig. 4c). The robust structure is associated with the carbon coating layer and hollow structure, which provides both mechanical support and electrical pathway, thus ensuring good cycling stability and fast rate capability.

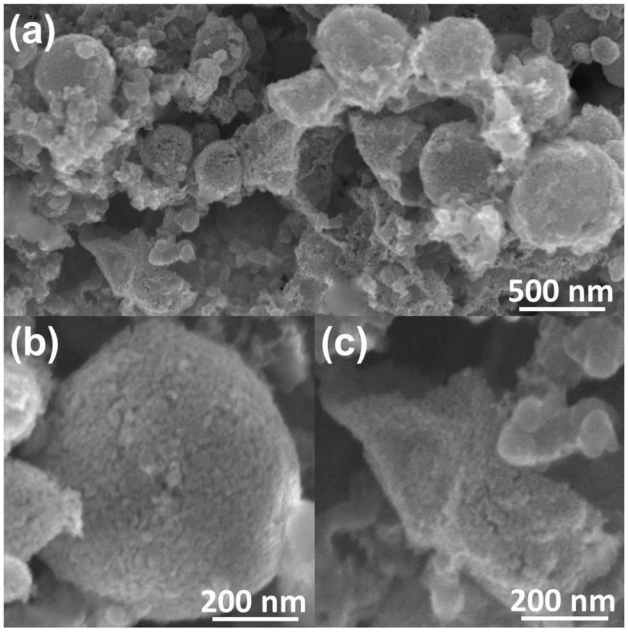

Fig. 4 SEM images of the nano-structured carbon-coated CuO hollow spherical particles after 70 charge/discharge cycles.

Conclusion

Carbon-coated CuO hollow spheres with a thin layer of CuO NPs anchored to the outer carbon layer were synthesized using a one-step, fast, scalable, and low-cost synthesis method, aerosol spray pyrolysis. The nano-structured carbon-coated CuO hollow spherical particles showed high capacity, long cycling stability, and excellent rate capability. The exceptional performance is attributed to the unique architecture of the carbon-coated CuO hollow spherical particles. This work provides a facile way to design and develop novel nano-structured electrode materials for high performance rechargeable batteries.

Acknowledgements

The authors gratefully acknowledge the support of the Army Research Office under contract no.: W911NF1110231. We acknowledge the support of the Maryland NanoCenter and its NispLab. The NispLab is supported in part by the NSF as a MRSEC Shared Experimental Facility.

References

1 U. Kasavajjula, C. S. Wang and A. J. Appleby, *J. Power Sources*, 2007, **163**, 1003.
2 M. V. Reddy, G. V. Subba Rao and B. V. R. Chowdari, *Chem. Rev.*, 2013, **113**, 5364.
3 W. Wei, Z. Wang, Z. Liu, Y. Liu, L. He, D. Chen, A. Umar, L. Guo and J. Li, *J. Power Sources*, 2013, **238**, 376.
4 P. Poizot, S. Laruelle, S. Grugeon, L. Dupont and J.-M. Tarascon, *Nature*, 2000, **407**, 496.

5 J. Cabana, L. Monconduit, D. Larcher and M. R. Palacín, *Adv. Mater.*, 2010, **22**, E170.
6 S.-F. Zheng, J.-S. Hu, L.-S. Zhong, W.-G. Song, L.-J. Wan and Y.-G. Guo, *Chem. Mater.*, 2008, **20**, 3617.
7 F.-S. Ke, L. Huang, G.-Z. Wei, L.-J. Xue, J.-T. Li, B. Zhang, S.-R. Chen, X.-Y. Fan and S.-G. Sun, *Electrochim. Acta*, 2009, **54**, 5825.
8 J. C. Park, J. Kim, H. Kwon and H. Song, *Adv. Mater.*, 2009, **21**, 803.
9 S. Ko, J. Lee, H. S. Yang, S. Park and U. Jeong, *Adv. Mater.*, 2012, **24**, 4451.
10 L. Wang, W. Cheng, H. Gong, C. Wang, D. Wang, K. Tang and Y. Qian, *J. Mater. Chem.*, 2012, **22**, 11297.
11 L. B. Chen, N. Lu, C. M. Xu, H. C. Yu and T. H. Wang, *Electrochim. Acta*, 2009, **54**, 4198.
12 J. Y. Xiang, J. P. Tu, J. Zhang, J. Zhong, D. Zhang and J. P. Cheng, *Electrochem. Commun.*, 2010, **12**, 1103.
13 M. A. Dar, S. H. Nam, Y. S. Kim and W. B. Kim, *J. Solid State Electrochem.*, 2010, **14**, 1719.
14 J. Zhou, L. Ma, H. Song, B. Wu and X. Chen, *Electrochem. Commun.*, 2011, **13**, 1357.
15 X. Chem, N. Zhang and K. Sun, *J. Mater. Chem.*, 2012, **22**, 13637.
16 L. Wang, H. Gong, C. Wang, D. Wang, K. Tang and Y. Qian, *Nanoscale*, 2012, **4**, 6850.
17 J. Lee, S. Choi and S. Park, *Chem.–Asian J.*, 2013, **8**, 1377.
18 Y. Ren, A. R. Armstrong, F. Jiao and P. G. Bruce, *J. Am. Chem. Soc.*, 2010, **132**, 996.
19 G. Q. Jian, L. Liu and M. R. Zachariah, *Adv. Funct. Mater.*, 2013, **23**, 1341.
20 A. Débart, L. Dupont, P. Poizot, J.-B. Leriche and J. M. Tarascon, *J. Electrochem. Soc.*, 2001, **148**, A1266.
21 Y. H. Xu, G. Q. Jian, Y. H. Liu, Y. J. Zhu, M. R. Zachariah and C. S. Wang, *Nano Energy*, 2014, **3**, 26.
22 X. H. Huang, C. B. Wang, S. Y. Zhang and F. Zhou, *Electrochim. Acta*, 2011, **56**, 6752.
23 Y. H. Xu, J. C. Guo and C. S. Wang, *J. Mater. Chem.*, 2012, **22**, 9562.
24 M. F. Hassan, M. M. Rahman, Z. P. Guo, Z. X. Chen and H. K. Liu, *Electrochim. Acta*, 2010, **55**, 5006.
25 S. Grugeon, S. Laruelle, L. Dupont and J.-M. Tarascon, *Solid State Sci.*, 2008, **5**, 895.
26 J. Y. Xiang, J. P. Tu, Y. Q. Qiao, X. L. Wang, J. Zhong, D. Zhang and C. D. Gu, *J. Phys. Chem. C*, 2011, **115**, 2505.